

Nonlinear optics

Anders Aspegren Søndergaard

Kristoffer Theis Skalmstang

Michael Munch

Steffen Videbæk Fredsgaard

February 28, 2014

Contents

Contents	1
1 Introduction	1
2 The Kerr effect	2
2.1 Mathematical details at a glance	2
2.2 Qualitative interpretation	2
2.3 Numerical work	3
3 Wave mixing	6

1 Introduction

During the better part of the course we have studied linear phenomena, that is the interaction between matter and light described by the wave equation

$$\nabla^2 \mathbf{E} - \frac{1}{c^2} \frac{\partial^2 \mathbf{E}}{\partial t^2} = \frac{1}{\epsilon_0 c^2} \frac{\partial^2 \mathbf{P}}{\partial t^2}, \quad (1)$$

where the polarization \mathbf{P} is linear wrt. the electric field of the light \mathbf{E} , as described by $\mathbf{P} = \epsilon_0 \chi \mathbf{E}$, where χ is electric susceptibility of the medium. The course has touched upon nonlinear phenomena, where the polarization can be expanded as $\mathbf{P} = \epsilon_0 (\chi^{(1)} \mathbf{E} + \chi^{(2)} \mathbf{E}^2 + \dots)$.

In this project we describe and discuss two such effects, namely beam self-focusing using the Kerr effect, and wave mixing.

2 The Kerr effect

The Kerr effect is found in media, where the index of refraction is dependent on the electric field of the propagating light. For real life laser beams, where the (time averaged) amplitude of electric field depends on the position in the beam, this leads to a index of refraction varying over the spacial position within the beam. Under certain and experimentally obtainable conditions, this leads to self-focusing of the beam within a passive medium.

2.1 Mathematical details at a glance

The mathematical formulation of the Kerr effect is derived in **milonni**. For a monochromatic laser field $E = \mathcal{E}e^{-i\omega t}$ with frequency ω in an isotropic and centrosymmetric medium (ie. a medium which quantum states have definite parity), an alternative wave equation for the complex laser field and polarization amplitudes is found. The most important point here is, that the polarization has a linear and a nonlinear contribution $\mathcal{P} = \mathcal{P}^L + \mathcal{P}^{NL}$:

$$\nabla^2 \mathcal{E} + \frac{\omega^2}{c^2} \mathcal{E} = -\frac{\omega^2}{\epsilon_0 c^2} \mathcal{P} = -\frac{\omega^2}{\epsilon_0 c^2} (\epsilon_0 \chi_1 \mathcal{E} + \epsilon_0 \chi_3 |\mathcal{E}|^2 \mathcal{E}). \quad (2)$$

It should be noted, that the susceptibilities here are not simple scalars, but are certain values of the nonlinear susceptibility tensor. For a monochromatic field, χ_1 and χ_3 are constant as ω is constant. Defining

$$-\chi \frac{\omega^2}{c^2} \mathcal{E} \equiv -\chi_1 \frac{\omega^2}{c^2} \mathcal{E} - \chi_3 \frac{\omega^2}{c^2} |\mathcal{E}|^2 \mathcal{E} \quad (3)$$

and using $n^2 = 1 + \chi$ leads to

$$n = \sqrt{1 + \chi_1 + \chi_3 |\mathcal{E}|^2} = n_0 \sqrt{1 + \frac{\chi_3}{n_0^2} |\mathcal{E}|^2} \quad (4)$$

$$\simeq n_0 + \frac{\chi_3}{2n_0} |\mathcal{E}|^2 \equiv n_0 + \frac{1}{2} n_2 |\mathcal{E}|^2, \quad (5)$$

where $n_0 = \sqrt{1 + \chi_1}$ is the linear refractive index in the medium. Clearly, the effective refractive index felt by the propagating wave, depends on the form of the electric field.

2.2 Qualitative interpretation

As shown i figure 1, a gaussian beam, which is a beam exhibiting cylindrical symmetry and where the intensity distribution is or nearly is gaussian, feels a larger refractive index closer to the beam axis. Eqn. (5) shows, that this nonlinear correction is proportional to the norm square of the field amplitude, ie. the beam intensity.

The beam size of an gaussian beam is not constant, but varies along the beam axis z , with minimum beam cross section found at the beam waist.

Fixme Warning:
Implicit
approximation:
feltet er ikke så
stærkt, at der
kræves højere
ordener.



Figure 1: Gaussisk beamprofil og effektivt brydningsindeks.

Using a geometric interpretation of the light, rays moving away from the waist have increasing distance from the axis, ie. radial distance r , leading to a broadening of the beam and a lower intensity. As such, the rays move from a region of high to lower refraction index, leading to a reflection of the ray back towards the beam axis.

This self-focusing competes with diffractive spreading and below a certain critical intensity, self-focusing is not observed. This limit is normally given in terms of total beam power, for example:

$$P_{\text{crit}}^{\text{gauss}} \sim \frac{c\epsilon_0}{8\pi} \frac{\lambda^2}{n_2} \quad \text{Gaussian beam [milonni]}, \quad (6)$$

$$P_{\text{crit}}^{\text{cyl}} \approx \frac{ca^2}{64} \frac{\lambda^2}{n_2} \quad \text{Cylindrical beam of uniform intensity [prl-selftrap]}, \quad (7)$$

where the angular diffractive divergence of the cylindrical beam is $a\lambda/n_0 2r$. Note here, that the critical power decreases linearly in n_2 but increases quadratically in wavelength.

In optics, media where this self-focusing is present are termed Kerr lenses, as the passive medium acts as a lens for beams passing through. The dioptric power (inverse focal length) of a Kerr lens of length z for a circular gaussian beam of power P with waist radius w_0 is [yefet-kerrlens]

$$f_{\text{kerr}}^{-1} = \frac{4}{\pi} \frac{n_2 P}{w_0^4} z. \quad (8)$$

2.3 Numerical work

We wish to confirm the numerical results from **prl-selffocus**, that is we wish to show, that a gaussian beam is focused when propagating in a Kerr lense.

The partial differential equation given in Eqn. (??) is categorized as a 1D diffusion problem. A method to solve this problem is the Crank-Nicolson method which applies for equations of the form

$$\frac{\partial u}{\partial t} = F\left(u, x, t, \frac{\partial u}{\partial x}, \frac{\partial^2 u}{\partial x^2}\right), \quad (9)$$

which is also the case for our equation, since it can be rewritten as

$$i \frac{\partial E}{\partial z} = -\frac{1}{2} \left[\frac{1}{r} \frac{\partial E}{\partial r} + \frac{\partial^2 E}{\partial r^2} + |E|^2 E \right]. \quad (10)$$

In order to evaluate this numerically we discretize z and r in order to make a grid. The first and second order derivatives can then be approximated by the central finite difference

$$f'(x) = \frac{f(x + \frac{1}{2}h) - f(x - \frac{1}{2}h)}{h} \quad f''(x) = \frac{f(x + h) - 2f(x) + f(x - h)}{h^2}. \quad (11)$$

The Crank-Nicolson method then relates the value of E at the $n + 1$ z-step to the value in the n 'th step via the equalities of the forward and backward euler method. Note that i denote the step in r

$$\frac{E_i^{n+1} - E_i^n}{\Delta z} = \frac{1}{2} [F_i^{n+1} + F_i^n]. \quad (12)$$

The right hand side of the can be evaluated using the central difference approximation. This gives a set of equations for E^{n+1} that depends on E^n ie. the values in the previous step

$$\begin{aligned} & (\alpha + 2\beta^2 - |E_i^{n+1}|^2)E_i^{n+1} - \beta^2(E_{i+2}^{n+1} + E_{i-2}^{n+1}) - \frac{\beta}{r_i}(E_{i+1}^{n+1} - E_{i-1}^{n+1}) \\ & = (\alpha - 2\beta^2 + |E_i^n|^2)E_i^n + \beta^2(E_{i+2}^n + E_{i-2}^n) + \frac{\beta}{r_i}(E_{i+1}^n - E_{i-1}^n), \end{aligned} \quad (13)$$

where $\alpha = -2i/\Delta z$ and $\beta = 1/2\Delta r$.

This is almost a fivediagonal matrix equation except for the term that is cubic in E_i^{n+1} . However with sufficiently small steps one can approximate the cubic term to be $|E_i^{n+1}|^2 E_i^{n+1} \approx |E_i^n|^2 E_i^{n+1}$ ie. take the quadratic part from the last step. In each timestep one must then solve the matrix inversion problem

$$\mathbf{A}\mathbf{E}^{n+1} = \mathbf{B}\mathbf{E}^n, \quad (14)$$

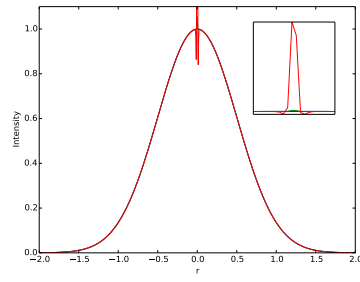
where the coefficients that make up these two matrices is the coefficients listed in Eqn. (13).

Results

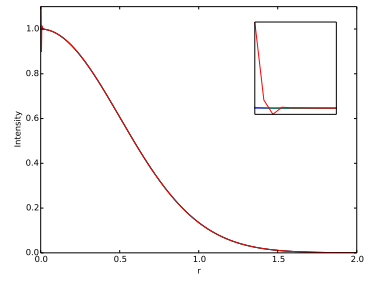
We have implemented the Crank-Nicolson algorithm in the Python language. The code can be found on <https://github.com/Munken/Laser>.

For the numerical simulation the boundary conditions it quite important. Since our beam is Gaussian we enforce that $E \rightarrow 0$ as $r \rightarrow \infty$. Furthermore the first derivative in $r = 0$ should be 0 since the beam is cylindrically symmetric.

We have tried to introduce these boundary conditions in two ways. Figure 2(a) shows a simulation where we have simulated on $\pm r$. Figure 2(b) shows the same simulation where we have only simulated from 0. It is clear from these two figures that we have numerical instabilities for the small r -values. We have not been able to solve this problem so we have not been able to reproduce [p_{rl}-selffocus] [Fig. 1].



(a) Symmetric



(b) Symmetric

Figure 2: The result of our numnerical simulation after propagating 10 steps. The insets shows the behavior around $r = 0$.

3 Wave mixing